
Unsupervised Learning for Quadratic Assignment

Yimeng Min

Department of Computer Science
Cornell University
Ithaca, NY, USA
min@cs.cornell.edu

Carla P. Gomes

Department of Computer Science
Cornell University
Ithaca, NY, USA
gomes@cs.cornell.edu

Abstract

We introduce PLUME search, a data-driven framework that enhances search efficiency in combinatorial optimization through unsupervised learning. Unlike supervised or reinforcement learning, PLUME search learns directly from problem instances using a permutation-based loss with a non-autoregressive approach. We evaluate its performance on the quadratic assignment problem, a fundamental NP-hard problem that encompasses various combinatorial optimization problems. Experimental results demonstrate that PLUME search consistently improves solution quality. Furthermore, we study the generalization behavior and show that the learned model generalizes across different densities and sizes.

1 Introduction

Combinatorial Optimization (CO) represents a central challenge in computer science and operations research, targeting optimal solutions within a large search space. CO encompasses numerous practical applications, including transportation logistics, production scheduling, network design, and resource allocation. The computational complexity of CO problems is typically NP-hard, making exact methods intractable for large instances. Researchers have thus developed approximation algorithms, heuristics, and hybrid approaches that balance solution quality with computational feasibility. These methods include simulated annealing, genetic algorithms, tabu search, and various problem-specific heuristics that can generate high-quality solutions within reasonable time budget Kirkpatrick et al. [1983], Holland [1992], Johnson and McGeoch [1997], Glover and Laguna [1998], Gomes and Selman [2001], Blum and Roli [2003].

1.1 Data-driven Combinatorial Optimization

Recently, data-driven methods have gained significant attention in addressing combinatorial optimization problems. Taking the Travelling Salesman Problem (TSP) as an example, researchers have explored both Supervised Learning (SL) and Reinforcement Learning (RL) methods. In SL, approaches such as pointer networks and graph neural networks attempt to learn mappings from problem instances to solutions by training on optimal or near-optimal tours Joshi et al. [2019], Vinyals et al. [2015]. These models learn to imitate optimal or near-optimal solutions, leading to significant computational expense when building the training dataset. RL approaches frame TSP as a sequential decision-making problem where an agent learns to construct tours in a Markov decision process framework. While RL models have shown promise in small instances, these methods face significant challenges when scaling to larger problems. Furthermore, the sparse rewards and the high variance during training make it difficult for RL agents to learn effective policies Bello et al. [2016].

An alternative approach is Unsupervised Learning (UL), which avoids sequential decision making and does not require labelled data. In Min et al. [2023], the authors propose a surrogate loss for the TSP objective by using a soft indicator matrix \mathbb{T} to construct the Hamiltonian cycle, which is

then optimized for minimum total distance. The \mathbb{T} operator can be essentially interpreted as a soft permutation operator, as demonstrated in Min and Gomes [2023], which represents a rearrangement of nodes on the route $1 \rightarrow 2 \rightarrow 3 \rightarrow \dots \rightarrow n \rightarrow 1$, with n representing the number of cities.

The TSP loss used in UL can be formally expressed in matrix notation. Essentially, we optimize:

$$\mathcal{L}_{\text{TSP}} = \langle \mathbb{T}\mathbb{V}\mathbb{T}^T, \mathbf{D}_{\text{TSP}} \rangle, \quad (1)$$

where \mathbb{V} represents a Hamiltonian cycle matrix encoding the route $1 \rightarrow 2 \rightarrow \dots \rightarrow n \rightarrow 1$, \mathbb{T} is an approximation of a hard permutation matrix \mathbf{P} , and \mathbf{D}_{TSP} is the distance matrix with self-loop distances set to λ . $\mathbb{T}\mathbb{V}\mathbb{T}^T$ is a heat map that represents the probability that each edge belongs to the optimal solution, which guides the subsequent search process.

Since permutation operators are ubiquitous across many CO problems, and the application to TSP demonstrates their effectiveness, here, we extend this approach to a broader class of problems. Specifically, we propose **Permutation-based Loss with Unsupervised Models for Efficient search (PLUME search)**, an unsupervised data-driven heuristic framework that leverages permutation-based learning to solve CO problems.

1.2 Quadratic Assignment Problem

The Quadratic Assignment Problem (QAP), essentially a permutation optimization problem, is an NP-hard problem with numerous applications across facility layout, scheduling, and computing systems. For example, in facility layout, QAP finds the optimal permutation of facilities minimizing total interaction costs based on inter-facility flows and inter-location distances. QAP’s applications also include manufacturing plant design, healthcare facility planning, VLSI circuit design, telecommunications network optimization, and resource scheduling Koopmans and Beckmann [1957], Lawler [1963].

Formally, QAP asks to assign n facilities to n locations while minimizing the total cost, which depends on facility interactions and location distances. A flow matrix $\mathbf{F} \in \mathbb{R}^{n \times n}$ captures the interaction cost between facility i and facility j . Each location is represented by a matrix $\mathbf{X} \in \mathbb{R}^{n \times 2}$, where each row contains the coordinates of a location. The distance matrix $\mathbf{D} \in \mathbb{R}^{n \times n}$ is computed using the Euclidean distance $\mathbf{D}_{ij} = \|\mathbf{X}_i - \mathbf{X}_j\|_2$.

The objective is to find a permutation matrix $\mathbf{P} \in \{0, 1\}^{n \times n}$ that maps facilities to locations while minimizing the total cost, given by $\min_{\sigma \in S_n} \sum_{i=1}^n \sum_{j=1}^n F_{ij} D_{\sigma(i), \sigma(j)}$, where σ is a permutation of $\{1, \dots, n\}$ defining the assignment and S_n denotes the set of all $n \times n$ permutation operators. This cost function can be equivalently written in matrix form as:

$$\min_{\mathbf{P} \in S_n} \langle \mathbf{P}\mathbf{F}\mathbf{P}^T, \mathbf{D} \rangle, \quad (2)$$

where \mathbf{P} is the permutation matrix representing the assignment.

1.3 Unsupervised Learning for QAP

In this paper, we use PLUME search to solve QAP. Following the TSP fashion in Min et al. [2023], we use neural networks (NNs) coupled with a Gumbel-Sinkhorn operator to construct a soft permutation matrix \mathbb{T} that approximates a hard permutation matrix \mathbf{P} . We use the soft permutation \mathbb{T} to guide the subsequent search process, as shown in Figure 1. PLUME search is a neural-guided

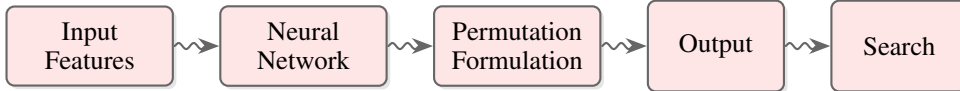


Figure 1: Overview of PLUME search framework: Input features are transformed through a neural network into a permutation formulation, then the output of the neural network guides the subsequent search process. This unified architecture allows PLUME to handle various combinatorial optimization problems by learning permutation operators.

heuristic that learns problem representations through NNs to directly guide the search. By integrating learned representations, PLUME search leverages UL to enhance search performance.

Here, for QAP, while TSP uses the heat map $\mathcal{H} = \mathbb{T}\mathbb{V}\mathbb{T}^T$ as a soft matrix (heat map) to guide the search, we directly decode a hard permutation matrix \mathbf{P} from \mathbb{T} . This permutation matrix \mathbf{P} represents an alignment in QAP and serves as an initialization to guide the subsequent search.

2 Tabu Search

We adopt Tabu search as the backbone of our PLUME search framework. Tabu Search (TS) is a method introduced by Glover Glover and Laguna [1998] that enhances local search methods by employing memory structures to navigate the solution space effectively. Unlike traditional hill-climbing algorithms, TS allows non-improving moves to escape local optima and uses adaptive memory to avoid cycling through previously visited solutions. The algorithm maintains a *tabu list* that prohibits certain moves, creating a dynamic balance between intensification and diversification strategies.

Tabu Search for Quadratic Assignment TS has emerged as one of the most effective meta-heuristics for addressing QAP instances Taillard [1991], Drezner [2003], James et al. [2009]. The algorithm navigates the solution space through strategic move evaluations and maintaining memory structures to prevent cycling and encourage diversification. For QAP, TS typically begins with a random permutation as the initial solution and employs a swap-based neighborhood structure where adjacent solutions are generated by exchanging the assignments of two facilities. A key component of TS is the tabu list, which records recently visited solutions or solution attributes to prevent immediate revisiting. In QAP implementations, the tabu list typically tracks recently swapped facility pairs, prohibiting their re-exchange for a specified number of iterations—the tabu tenure. This memory structure forces the search to explore new regions of the solution space even when immediate improvements are not available, helping the algorithm escape local optima. The performance depends mainly on three parameters: `neighbourhoodSize`, which controls the sampling density from the complete swap neighbourhood at each iteration; `evaluations`, which establishes the maximum computational budget as measured by objective function calculations; and `maxFails`, which implements an adaptive early termination criterion that halts the search after a predefined number of consecutive non-improving iterations. Together, these parameters balance exploration breadth against computational efficiency, ensuring both effective solution space coverage and predictable runtime performance Glover [1989], Blum and Roli [2003], Battiti and Tecchiolli [1994], Misevicius [2005].

3 Model

We design NNs that preserve permutation equivalence while effectively encoding the underlying structure of QAP. Specifically, our NNs preserve permutation equivariance to ensure consistent handling of isomorphic problem instances. Furthermore, our model generalizes across variable problem sizes without modifying the NNs.

3.1 Permutation-Equivariant QAP Architecture

The NN’s structure is shown in Figure 2. Our permutation-equivariant architecture has two inputs: node positions $\mathbf{X} \in \mathbb{R}^{n \times 2}$ representing 2D coordinates and flow matrices $\mathbf{F} \in \mathbb{R}^{n \times n}$ representing pairwise interactions, where n is the number of facilities. Our model consists of three main components: a position encoder, two flow feature encoders, and the main network. The position encoder maps facility coordinates through a shared Multi-Layer Perceptron (MLP) ϕ_{pos} to embed spatial information, the flow encoders process row-wise and column-wise interactions through pooling operations and MLPs:

$$\mathbf{H}_{\text{pos}} = \phi_{\text{pos}}(\mathbf{X}), \quad \mathbf{H}_{\text{row}} = \psi_{\text{row}} \left(\sum_{j=1}^N \phi_{\text{row}}(\mathbf{F}_{ij}) \right), \quad \mathbf{H}_{\text{col}} = \psi_{\text{col}} \left(\sum_{i=1}^N \phi_{\text{col}}(\mathbf{F}_{ij}) \right), \quad (3)$$

where $\phi_{\text{row}}, \phi_{\text{col}} : \mathbb{R} \rightarrow \mathbb{R}^d$ and $\phi_{\text{pos}} : \mathbb{R}^2 \rightarrow \mathbb{R}^d$ are MLPs that transform input features into d -dimensional latent representations, and $\psi_{\text{row}}, \psi_{\text{col}} : \mathbb{R}^d \rightarrow \mathbb{R}^d$ are MLPs that process the aggregated features to capture facility interactions. These features are concatenated and processed through L

permutation-equivariant MLP layers before the final projection:

$$\mathbf{H}^{(0)} = [\mathbf{H}_{\text{pos}} \parallel \mathbf{H}_{\text{row}} \parallel \mathbf{H}_{\text{col}}], \quad \mathbf{H}^{(\ell+1)} = \text{MLP}^{(\ell)}(\mathbf{H}^{(\ell)}), \quad \mathbf{Y} = \Theta \mathbf{H}^{(L)}, \quad (4)$$

where $\mathbf{H}^{(0)} \in \mathbb{R}^{n \times 3d}$ contains the concatenated initial node features, $\mathbf{H}^{(\ell)}$ represents node embeddings at layer ℓ , and $\text{MLP}^{(\ell)}$ denotes the ℓ -th layer. These MLPs map from $3d$ to d dimensions, while the final linear layer $\Theta \in \mathbb{R}^{d \times m}$ projects from d to m dimensions. $\mathbf{Y} \in \mathbb{R}^{n \times m}$ is the final output logits for assignment prediction. This architecture preserves permutation equivariance, that is, $f(\Pi \mathbf{X}, \Pi \mathbf{F} \Pi^T) = \Pi f(\mathbf{X}, \mathbf{F})$ for any permutation matrix $\Pi \in S_n$, where f represents the network function mapping inputs \mathbf{X}, \mathbf{F} to output \mathbf{Y} .

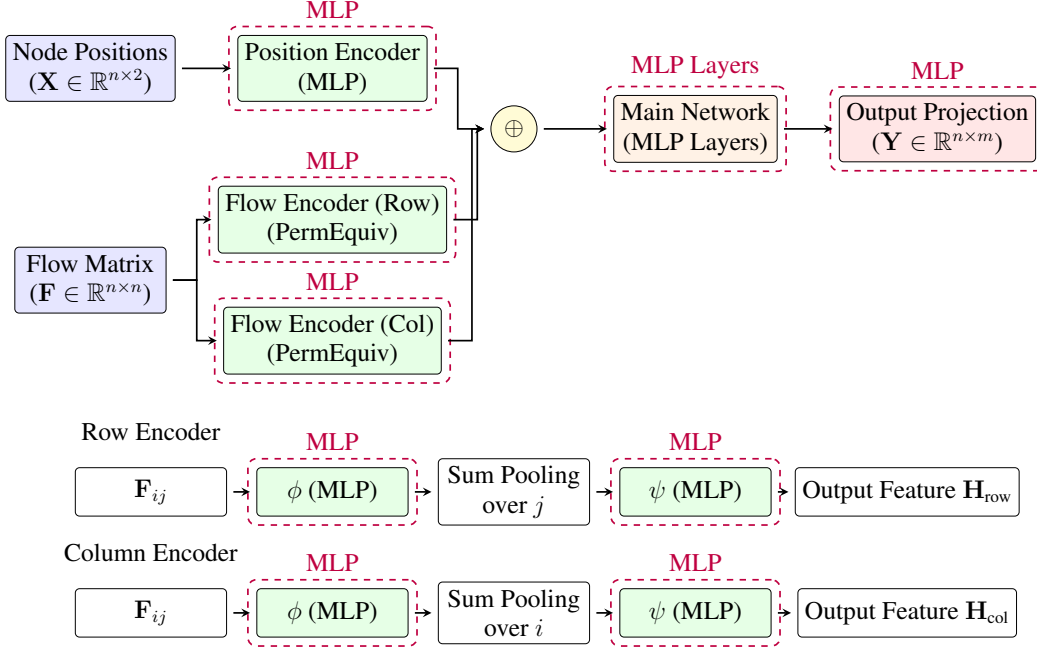


Figure 2: Neural network architecture for QAP. The model takes coordinates and flow matrix data and passes them into MLP encoders, the resulting features are then concatenated together. We then feed them into the main network and generate \mathbf{Y} through an output layer.

3.2 Building Soft Permutation \mathbb{T}

Our model first generates logits which are transformed by a scaled hyperbolic tangent activation:

$$\mathcal{F} = \alpha \tanh(\mathbf{Y} \mathbf{Y}^T), \quad (5)$$

where α is a scaling parameter that controls the magnitude of the output. We then construct a soft permutation matrix \mathbb{T} using the Gumbel-Sinkhorn operator:

$$\mathbb{T} = \text{GS}\left(\frac{\mathcal{F} + \gamma \times \text{Gumbel noise}}{\tau}, l\right), \quad (6)$$

where GS denotes the Gumbel-Sinkhorn operator that builds a continuous relaxation of a permutation matrix. Here, γ controls the scale of the Gumbel noise which adds stochasticity to the process, τ is the temperature parameter that controls the sharpness of the relaxation (lower values approximate discrete permutations more closely), and l is the number of Sinkhorn normalization iterations.

During inference, we obtain a discrete permutation matrix \mathbf{P} by applying the Hungarian algorithm to the scaled logits: $\mathbf{P} = \text{Hungarian}\left(-\frac{\mathcal{F} + \gamma \times \text{Gumbel noise}}{\tau}\right)$. We use the CUDA implementation of the batched linear assignment solver for the Hungarian operator from Karpukhin et al. [2024].

3.3 Invariance Property of Permutation Representation

The soft permutation matrix \mathbb{T} is constructed through Equations 5 and 6 to preserve permutation equivariance. Let $\Pi \in S_n$ represent a random permutation on the nodes, the distance and flow matrices transform as $\mathbf{D} = \Pi \mathbf{D}_0 \Pi^T$ and $\mathbf{F} = \Pi \mathbf{F}_0 \Pi^T$, where \mathbf{D}_0 and \mathbf{F}_0 are the distance matrix and flow matrix before this random permutation respectively. Now, let \mathbf{Y}_0 denote the initial output, given that the network output transforms under permutation Π as $\mathbf{Y} = \Pi \mathbf{Y}_0$, we then have $\mathbb{T} = \Pi \mathbb{T}_0 \Pi^T$. Consequently, the objective function $\langle \mathbb{T} \mathbf{F} \mathbb{T}^T, \mathbf{D} \rangle$ remains invariant. To be specific, $\forall \Pi \in S_n$, we have:

$$\begin{aligned} \langle \mathbb{T} \mathbf{F} \mathbb{T}^T, \mathbf{D} \rangle &= \langle \Pi \mathbb{T}_0 \Pi^T \left(\Pi \mathbf{F}_0 \Pi^T \right) \left(\Pi \mathbb{T}_0 \Pi^T \right)^T, \Pi \mathbf{D}_0 \Pi^T \rangle \\ &= \langle \Pi \mathbb{T}_0 \underbrace{\Pi^T \Pi}_{=I} \mathbf{F}_0 \underbrace{\Pi^T \Pi}_{=I} \mathbb{T}_0^T \Pi^T, \Pi \mathbf{D}_0 \Pi^T \rangle = \langle \Pi \mathbb{T}_0 \mathbf{F}_0 \mathbb{T}_0^T \Pi^T, \Pi \mathbf{D}_0 \Pi^T \rangle \quad (7) \\ &= \langle \Pi \left(\mathbb{T}_0 \mathbf{F}_0 \mathbb{T}_0^T \right) \Pi^T, \Pi \mathbf{D}_0 \Pi^T \rangle = \langle \mathbb{T}_0 \mathbf{F}_0 \mathbb{T}_0^T, \mathbf{D}_0 \rangle. \end{aligned}$$

This invariance property guarantees consistent solutions for isomorphic problem instances. Overall, Equations 5 and 6 preserve permutation symmetry while enabling gradient-based optimization, with the additional benefit of allowing the model to naturally generalize across different problem sizes. This generalization capability arises because the soft permutation matrix $\mathbb{T} \in \mathbb{R}^{n \times n}$ always matches the input graph size, independent of the model’s parameters. Consequently, our approach scales to problems of varying sizes without needing to modify the NN.

4 Results

4.1 Data Generation

We generate synthetic instances using an Erdős-Rényi (ER) graph model following Tan and Mu [2024]. To build a QAP instance of size n , we generate a flow matrix $\mathbf{F} \in \mathbb{R}^{n \times n}$ and the location coordinates $\mathbf{X} = (\text{Uniform}(0, 1), \text{Uniform}(0, 1))$. We generate uniformly random weights in $[0, 1]$ for the upper triangular portion of \mathbf{F} , then mirror these values to create a symmetric matrix. We apply an ER graph mask with edge probability p to control the sparsity of connections between facilities.

Formally, for each QAP instance i :

$$\mathbf{F}_{ij} = \begin{cases} \text{Uniform}(0, 1) & \text{if } \text{rand}() < p \text{ and } i \neq j, \quad \forall i < j \\ 0 & \text{otherwise} \end{cases}, \quad (8)$$

$$\mathbf{F}_{ji} = \mathbf{F}_{ij}, \quad \forall i < j. \quad (9)$$

We build datasets with varying problem sizes $n \in \{100, 200\}$ and graph densities $p \in \{0.1, 0.2, \dots, 0.9\}$. For each configuration, we generate 30,000 instances for training, 5,000 for validation and 5,000 for test, respectively. We run experiments using an NVIDIA H100 GPU and an Intel Xeon Gold 6154 CPU.

4.2 Training

We optimize our NNs to minimize the QAP objective:

$$\langle \mathbb{T} \mathbf{F} \mathbb{T}^T, \mathbf{D} \rangle, \quad (10)$$

with the model’s hidden dimension set to either 32 or 64. The number of layers l is set to either 2 or 4. For the Gumbel-Softmax operator used in Equation 5, we set $\tau \in \{1, 2, 3, 4, 5\}$ and $l \in \{10, 20, 30, 40, 50\}$. The noise scale γ is set to either 0.001 or 0.01. The \tanh scale is set to $\alpha = 40$. We use the Adam optimizer with a learning rate of 3×10^{-5} and train for 100 epochs. We then select the model with the best validation performance to evaluate on the test set. For problem size 100, we set $m = 100$, and for problem size 200, we set $m = 200$.

4.3 Method

We train our model on each problem size n and each graph density p . After training the model, we then validate it and select the best parameters before testing. We implement a PLUME search in a straightforward way. As mentioned, the model outputs the soft permutation matrix \mathbb{T} , and we decode the hard permutation matrix \mathbf{P} from \mathbb{T} . \mathbf{P} corresponds to a learned assignment. We then start the tabu search for QAP using this learned assignment as the initial solution.

Table 1: Comparison between the average costs of UL predicted solutions and random solutions. The gap value indicates the average percentage improvement of the predicted solution over the random solution’s cost. Inference time denotes the average total time (running NN inference+Hungarian) required to build the UL predicted solutions.

p	$n = 100$				$n = 200$			
	UL	random	Gap (%)	Inference (ms)	UL	random	Gap (%)	Inference (ms)
0.1	230.086	257.877	10.7768	2.80944×10^{-2}	958.645	1037.01	7.55682	1.91477×10^{-1}
0.2	478.116	515.381	7.23057	3.14968×10^{-2}	1968.86	2074.41	5.08819	1.82030×10^{-1}
0.3	730.449	773.459	5.56073	2.98188×10^{-2}	2987.00	3110.27	3.96332	1.96343×10^{-1}
0.4	984.907	1031.92	4.55588	3.15542×10^{-2}	4009.58	4144.96	3.26614	1.93695×10^{-1}
0.5	1239.22	1288.90	3.85445	2.83198×10^{-2}	5040.71	5184.32	2.77008	1.92888×10^{-1}
0.6	1496.41	1547.62	3.30895	2.83606×10^{-2}	6072.39	6219.82	2.37033	1.86270×10^{-1}
0.7	1754.76	1805.83	2.82806	3.20354×10^{-2}	7112.34	7257.90	2.00554	1.91129×10^{-1}
0.8	2025.43	2064.49	1.89199	2.93868×10^{-2}	8154.81	8298.41	1.73045	1.93583×10^{-1}
0.9	2278.93	2320.06	1.77280	2.78900×10^{-2}	9199.26	9336.99	1.47510	1.89588×10^{-1}
Mean	1246.48	1289.50	3.33618	2.96619×10^{-2}	5055.96	5184.90	2.48684	1.90778×10^{-1}

4.4 Effectiveness of UL-Based Initialization

Before diving into the PLUME search’s final results, we first check whether the learned assignment improves the solution quality without any subsequent search. We directly compare the quality of solutions using learned assignments versus random assignments in the initialization stage.

Table 1 demonstrates the cost of using UL-predicted solutions compared to random initialization. We define the gap as:

$$1 - \frac{\langle \mathbf{P}\mathbf{F}\mathbf{P}^T, \mathbf{D} \rangle}{\langle \mathbf{P}_{random}\mathbf{F}\mathbf{P}_{random}^T, \mathbf{D} \rangle},$$

where \mathbf{P} is the learned assignment and \mathbf{P}_{random} is a random assignment. The gap percentage shows consistent improvement across all problem densities, with more significant gains observed in sparser problems. For $n = 100$ with density $p = 0.1$, the UL approach achieves a 10.7770% improvement over random initialization, while for $n = 200$, it yields a 7.55672% improvement. As problem density increases, the gap narrows but remains positive, indicating that our approach maintains its advantage even for denser problems.

4.5 PLUME Search for QAP

We then run tabu search using different initializations. Tables 2 and 3 show the performance of PLUME tabu search compared with tabu search with random initialization. Our experimental results demonstrate that our UL-based method effectively solves QAPs. The solutions consistently outperform random initialization across all problem sizes and density parameters. Specifically, we vary the evaluations μ , neighbourhoodSize κ , maxFails ω and test PLUME search. We show that our UL-based initialization consistently outperforms random initialization within each parameter set, and the solution quality improves with increased evaluations μ . The performance gap is particularly pronounced in sparse problems (low p values), where for $p = 0.1$ and $n = 100$, PLUME search yields a 1.13662% improvement and on $p = 0.1$ and $n = 200$, PLUME search yields a 2.20771% improvement. This improvement gradually decreases as problem density increases, suggesting that our neural networks more effectively capture structural patterns in sparse problems.

Table 2: Performance comparison of algorithms on QAP instances with $n = 100$. $\text{TS}(\mu, \kappa, \omega)$ denotes the tabu search with evaluations : μ , neighbourhoodSize : κ , and maxFails : ω .

$\text{TS}(\mu, \kappa, \omega)$	$\text{TS}(1k, 25, 25)$		$\text{TS}(1k, 100, 25)$		$\text{TS}(1k, 25, 100)$		$\text{TS}(5k, 100, 100)$		$\text{TS}(10k, 100, 100)$	
p	UL	random	UL	random	UL	random	UL	random	UL	random
0.1	190.129	198.931	205.433	224.427	190.154	198.888	175.675	181.297	165.349	167.250
0.2	422.156	434.907	443.269	469.997	422.089	434.915	478.116	410.615	388.068	390.903
0.3	663.959	679.353	688.723	720.382	663.984	679.369	640.422	650.792	623.827	627.494
0.4	911.248	928.427	938.500	973.599	911.228	928.329	885.413	896.848	867.245	871.310
0.5	1160.92	1179.51	1189.85	1227.30	1161.02	1179.49	1133.85	1146.22	1114.71	1119.23
0.6	1415.86	1435.01	1445.24	1484.27	1415.84	1435.06	1387.92	1400.88	1368.54	1373.03
0.7	1673.38	1692.78	1703.09	1742.15	1673.31	1692.70	1645.29	1658.21	1625.78	1630.24
0.8	1939.07	1953.37	1972.66	2001.89	1939.01	1953.46	1910.17	1919.61	1889.13	1892.27
0.9	2198.54	2213.92	2229.21	2260.26	2198.55	2213.89	2171.44	2181.57	2152.00	2155.33
Average	1175.03	1190.69	1201.78	1233.81	1175.021	1190.68	1150.26	1160.67	1132.74	1136.34

Table 3: Performance comparison of algorithms on QAP instances with $n = 200$. $\text{TS}(\mu, \kappa, \omega)$ denotes the tabu search with evaluations : μ , neighbourhoodSize : κ , and maxFails : ω .

$\text{TS}(\mu, \kappa, \omega)$	$\text{TS}(1k, 25, 25)$		$\text{TS}(1k, 100, 25)$		$\text{TS}(1k, 25, 100)$		$\text{TS}(5k, 100, 100)$		$\text{TS}(10k, 100, 100)$	
p	UL	random	UL	random	UL	random	UL	random	UL	random
0.1	874.188	918.224	915.225	981.426	874.146	918.342	836.399	871.458	798.478	816.504
0.2	1851.52	1913.14	1908.32	1998.87	1851.68	1912.98	1799.74	1849.18	1748.06	1773.71
0.3	2848.72	2921.98	2987.00	3022.16	2848.77	2921.71	2788.05	2847.12	2727.83	2758.39
0.4	3856.81	3937.86	3929.77	4048.26	3856.62	3937.92	3790.02	3856.20	3724.59	3758.61
0.5	4878.52	4965.70	4955.69	5082.12	4878.88	4965.68	4807.95	4879.02	4738.94	4776.09
0.6	5905.06	5994.81	5984.58	6114.63	5905.33	5994.91	5832.49	5905.84	5761.67	5800.11
0.7	6943.11	7032.42	7023.56	7152.33	6943.24	7032.42	6869.62	6942.84	6798.78	6836.88
0.8	7988.29	8076.76	8067.27	8194.76	7988.28	8077.04	7916.56	7988.74	7846.75	7884.92
0.9	9039.82	9125.34	9115.28	9237.99	9040.02	9124.94	8971.13	9041.09	8904.87	8941.46
Average	4909.56	4987.36	4979.41	5092.50	4909.66	4987.33	4845.77	4909.06	4783.33	4816.30

Notably, the relative improvement from using PLUME search is more significant for larger problem sizes, with $n = 200$ showing consistently higher percentage improvements than $n = 100$ at comparable densities. This trend holds for tabu search with different parameters. For example, with parameters $\mu = 1,000$, $\kappa = 25$, and $\omega = 25$, the tabu search with random initialization achieves 1190.69 on average for $n = 100$, while PLUME search achieves 1175.03, yielding a 1.31520% improvement. At $n = 200$, PLUME search achieves 4909.56 on average while random initialized tabu search achieves 4987.36, resulting in a more substantial 1.55994% improvement. The most intensive tabu search configuration, $\text{TS}(10k, 100, 100)$, provides the most comprehensive exploration of the solution space and thus yields the best solution quality across all initialization methods. At this parameter setting, PLUME search further improves solution quality. For graphs with $n = 100$, PLUME search achieves an average solution cost of 1132.74 compared to 1136.34 for random initialization, yielding a 0.316807% improvement. While this may appear modest, it is important to note that as search parameters increase, the final solutions converge closer to optimality, leaving less room for improvement. The fact that PLUME search maintains its advantage even in this setting underscores the quality of its initialization. For larger graphs with $n = 200$ vertices, the benefit becomes more pronounced. PLUME search achieves an average cost of 4783.33 compared to 4816.30 for random initialization, yielding a 0.684550% improvement. This increasing advantage with problem size suggests that PLUME search scales well to larger problems.

Tables 4 and 5 show the execution time comparison (TS runtime) between random and UL-based initialization approaches for tabu search. The inference time for generating UL-predicted solutions is negligible: $< 3 \times 10^{-2}$ ms for $n = 100$ and $< 2 \times 10^{-1}$ ms for $n = 200$ (shown in Table 1). When accounting for both inference and execution time, the total computational cost of UL-based initialization remains comparable to random initialization across all parameter configurations. Overall, our results show that PLUME search effectively improves the efficiency of the tabu search algorithm, enabling the discovery of better solutions within a similar computational budget.

Table 4: Average Time comparison of tabu search with different search parameters on QAP instances with $n = 100$, in ms ($\times 10^{-3}$ s).

TS(μ, κ, ω)	TS(1k, 25, 25)		TS(1k, 100, 25)		TS(1k, 25, 100)		TS(5k, 100, 100)		TS(10k, 100, 100)	
p	UL	random	UL	random	UL	random	UL	random	UL	random
0.1	1.55014	1.47786	2.65438	2.01335	2.02096	2.32776	3.96913	3.86332	6.89681	6.40729
0.2	1.40809	1.72910	2.16947	2.11550	2.19710	2.13621	4.38935	4.10793	6.19193	6.92497
0.3	2.23220	2.30824	2.32095	2.20613	2.03746	2.12630	4.06415	4.28922	6.34255	6.50180
0.4	2.72354	2.91837	2.04465	2.24711	1.91479	2.45331	4.05188	4.01972	6.73373	6.90415
0.5	2.57762	1.60781	2.13888	2.35198	1.97659	2.44347	4.20058	4.24511	6.87188	6.36137
0.6	1.90425	1.71858	2.26572	2.21770	2.34254	1.99306	3.86804	3.87752	6.63121	6.72185
0.7	1.60661	1.57086	2.11504	2.34658	2.11745	2.13709	3.66044	3.91046	6.60751	6.77780
0.8	1.91665	2.06804	2.02229	2.31294	2.28833	1.97817	3.77077	3.66541	6.81585	6.88984
0.9	2.42608	2.11719	2.11124	2.00790	2.31411	2.31984	3.67512	4.25899	6.28867	6.47949
Mean	2.03835	1.94623	2.20474	2.20213	2.13437	2.21280	3.96105	4.02641	6.59779	6.66317

Table 5: Average Time comparison of tabu search with different search parameters on QAP instances with $n = 200$, in ms ($\times 10^{-3}$ s).

TS(μ, κ, ω)	TS(1k, 25, 25)		TS(1k, 100, 25)		TS(1k, 25, 100)		TS(5k, 100, 100)		TS(10k, 100, 100)	
p	UL	random	UL	random	UL	random	UL	random	UL	random
0.1	2.42600	2.29224	2.26313	2.38713	2.49597	2.70196	6.85827	6.82996	11.8025	11.8930
0.2	2.29030	2.33664	2.38857	2.28357	2.78697	2.75465	6.62369	6.64074	11.9798	11.8780
0.3	2.34508	2.32658	2.27949	2.36495	2.65163	2.77468	6.49103	6.87804	11.9024	11.7376
0.4	2.18291	2.57973	2.33208	2.16072	2.85288	2.80369	6.79153	6.76758	12.0805	11.9279
0.5	2.34563	2.22272	2.54632	2.50635	2.74198	2.82831	6.59106	6.78405	12.0350	11.9095
0.6	2.54630	2.29580	2.33564	2.56085	2.54337	2.97725	6.65846	6.81566	12.0519	11.6976
0.7	2.27941	2.27283	2.54844	2.33566	2.48008	3.13651	7.27975	7.16379	12.1370	11.8553
0.8	2.35310	2.39341	2.60996	2.48153	2.37177	2.01584	7.05032	6.80656	11.6703	11.8593
0.9	2.18062	2.51180	2.41696	2.68309	2.06515	2.72407	7.16032	7.26328	11.6522	11.5438
Mean	2.32771	2.35908	2.41340	2.41821	2.55442	2.74633	6.83383	6.88330	11.92351	11.81135

4.6 Compared with Other Data-driven Methods

We compare with recent work by Tan and Mu [2024], where the authors use RL and test only on QAP instances up to size 100. We run their model on $n = 100$ and $p = 0.7$, using their model, we observe an average cost of 1644.37 with an average time of ≈ 150 ms, our PLUME TS(10k, 100, 100) achieves better performance with a cost of 1625.78. Notably, our methods are substantially faster, with average time costs of just 7 ms. It should be noted that although Tan and Mu [2024] also uses tabu search as a benchmark; they employ a Python implementation, which is not as computationally efficient as our C++ implementation of tabu search. We didn't fine-tune the RL method and fine-tuning may yield better performance. However, the gaps are so dramatically large that even with optimization, the RL approach would remain substantially inferior.

5 Generalization

5.1 Cross-density Generalization

We further study how the model generalizes across different densities, as shown in Table 6 and 7. Using models trained on a specific edge density ($p = 0.7$), our results show the best performance on nearby densities ($p = 0.6$ and $p = 0.8$). Model performance gradually declines as we move further from the training density, with more significant drops at the extreme values ($p = 0.1$ and $p = 0.9$). This suggests the model captures transferable structural patterns that work best within a reasonable proximity to its training conditions. This effect is more pronounced with TS(1k, 25, 25) compared to configurations with more extensive search parameters. On $n = 100$, with TS(1k, 25, 25), the performance difference between PLUME and random initialization at $p = 0.6$ is 0.450171%, while with TS(10k, 100, 100), the difference narrows to 0.102693%.

Table 6: Generalization across densities for the model trained on $n = 100$, $p = 0.7$ and test on $n = 100$ with different densities. Random initialization shows costs using random initial assignments. UL-based initialization shows costs using assignments predicted by our neural network. $\text{TS}(\mu, \kappa, \omega)$ shows costs after running tabu search from random initialization. PLUME $\text{TS}(\mu, \kappa, \omega)$ shows costs after running tabu search from UL-predicted initialization.

Density	0.1	0.2	0.3	0.4	0.5	0.6	0.8	0.9
Random Initialization	257.877	515.381	773.459	1031.92	1288.90	1547.62	2064.49	2320.06
UL-based Initialization	258.090	515.928	774.288	1032.26	1282.81	1528.17	2049.10	2320.75
$\text{TS}(1k, 25, 25)$	198.931	434.907	679.353	928.427	1179.51	1435.01	1953.37	2213.92
PLUME $\text{TS}(1k, 25, 25)$	198.991	434.811	679.407	928.081	1177.45	1428.55	1947.81	2213.91
$\text{TS}(10k, 100, 100)$	167.250	390.903	627.494	871.310	1119.23	1373.03	1892.27	2155.33
PLUME $\text{TS}(10k, 100, 100)$	167.296	390.828	627.470	871.144	1118.73	1371.62	1891.02	2155.40

Table 7: Generalization across densities for the model trained on $n = 200$, $p = 0.7$ and test on $n = 200$ with different densities.

Density	0.1	0.2	0.3	0.4	0.5	0.6	0.8	0.9
Random Initialization	1037.01	2074.41	3110.27	4144.96	5184.32	6219.82	8298.41	9336.99
UL-based Initialization	1036.78	1968.86	3110.34	4199.06	5040.71	6072.39	8284.74	9358.93
$\text{TS}(1k, 25, 25)$	918.299	1913.04	2921.80	3937.95	4965.65	5994.98	8076.76	9125.18
PLUME $\text{TS}(1k, 25, 25)$	918.402	1851.55	2921.83	3965.58	4878.55	5905.10	8069.67	9137.63
$\text{TS}(10k, 100, 100)$	816.661	1773.70	2758.83	3758.61	4776.40	5800.17	7884.66	8941.58
PLUME $\text{TS}(10k, 100, 100)$	816.572	1748.18	2758.66	3768.02	4738.89	5761.62	7882.97	8946.10

5.2 Cross-size Generalization

Our model naturally generalizes across problem sizes due to its permutation-equivariant design, where the soft permutation matrix $\mathbb{T} \in \mathbb{R}^{n \times n}$ automatically adapts to match input dimensions. Experiments show that a model trained on $n = 100$ effectively generalizes to $n = 200$ problems and vice versa, while consistently outperforming random initialization, as shown in Table 8 and Table 9. For instance, when a model trained on $n = 200$ is applied to $n = 100$ problems, UL initialization achieves a solution cost of 1795.57 compared to 1805.83 for random initialization, and when used with $\text{TS}(1k, 25, 25)$, PLUME TS reaches 1688.43 versus 1692.78 for standard TS with random initialization.

6 Conclusion

In this paper, we propose PLUME search, a framework to enhance combinatorial optimization through UL. By leveraging permutation-based loss, we demonstrate that neural networks can effectively learn QAP directly from instances instead of using SL/RL. Our experimental results suggest that UL can generate high-quality initial solutions that significantly outperform random initialization and these better starting points consistently lead to better final solutions after tabu search. This is achieved by a simple NN structure with negligible computational overhead. Our approach demonstrates strong generalization across varying problem densities and sizes.

Table 8: Cross-size generalization: Model trained on $n = 200$ instances and tested on $n = 100$ instances (both with density $p = 0.7$). Random Initialization shows cost from random assignments; UL-based Initialization shows cost from UL model. $\text{TS}(\mu, \kappa, \omega)$ shows costs after running tabu search from random initialization. PLUME $\text{TS}(\mu, \kappa, \omega)$ shows costs after running tabu search from UL-predicted initialization.

Random Initialization	UL-based Initialization	TS (1k, 25, 25)	PLUME TS (1k, 25, 25)	TS (10k, 100, 100)	PLUME TS (10k, 100, 100)
1805.83	1795.57	1692.78	1688.43	1630.24	1629.54

Table 9: Cross-size generalization: Model trained on $n = 100$ instances and tested on $n = 200$ instances (both with density $p = 0.7$).

Random Initialization	UL-based Initialization	TS (1k, 25, 25)	PLUME TS (1k, 25, 25)	TS (10k, 100, 100)	PLUME TS (10k, 100, 100)
7257.90	7233.49	7023.566	7015.50	6836.88	6830.74

PLUME search takes a different approach from traditional heuristics and other SL/RL methods, offering a complementary method that integrates seamlessly with existing frameworks rather than competing with them. Future work might explore extending this approach to other permutation-based combinatorial problems, developing more sophisticated neural architectures to capture problem structure, and investigating the theoretical foundations of UL for combinatorial optimization.

7 Acknowledgement

This project is partially supported by the Eric and Wendy Schmidt AI in Science Postdoctoral Fellowship, a Schmidt Futures program; the National Science Foundation (NSF) and the National Institute of Food and Agriculture (NIFA); the Air Force Office of Scientific Research (AFOSR); the Department of Energy; and the Toyota Research Institute (TRI).

References

- Scott Kirkpatrick, C Daniel Gelatt Jr, and Mario P Vecchi. Optimization by simulated annealing. *science*, 220(4598):671–680, 1983.
- John H Holland. *Adaptation in natural and artificial systems: an introductory analysis with applications to biology, control, and artificial intelligence*. MIT press, 1992.
- David S Johnson and Lyle A McGeoch. The traveling salesman problem: a case study. *Local search in combinatorial optimization*, pages 215–310, 1997.
- Fred Glover and Manuel Laguna. *Tabu search*. Springer, 1998.
- Carla P Gomes and Bart Selman. Algorithm portfolios. *Artificial Intelligence*, 126(1-2):43–62, 2001.
- Christian Blum and Andrea Roli. Metaheuristics in combinatorial optimization: Overview and conceptual comparison. *ACM computing surveys (CSUR)*, 35(3):268–308, 2003.
- Chaitanya K Joshi, Thomas Laurent, and Xavier Bresson. An efficient graph convolutional network technique for the travelling salesman problem. *arXiv preprint arXiv:1906.01227*, 2019.
- Oriol Vinyals, Meire Fortunato, and Navdeep Jaitly. Pointer networks. *Advances in neural information processing systems*, 28, 2015.
- Irwan Bello, Hieu Pham, Quoc V Le, Mohammad Norouzi, and Samy Bengio. Neural combinatorial optimization with reinforcement learning. *arXiv preprint arXiv:1611.09940*, 2016.
- Yimeng Min, Yiwei Bai, and Carla P Gomes. Unsupervised learning for solving the travelling salesman problem. *Advances in Neural Information Processing Systems*, 36:47264–47278, 2023.
- Yimeng Min and Carla Gomes. Unsupervised learning permutations for tsp using gumbel-sinkhorn operator. In *NeurIPS 2023 Workshop Optimal Transport and Machine Learning*, 2023.
- Tjalling C Koopmans and Martin Beckmann. Assignment problems and the location of economic activities. *Econometrica: journal of the Econometric Society*, pages 53–76, 1957.
- Eugene L Lawler. The quadratic assignment problem. *Management science*, 9(4):586–599, 1963.
- Éric Taillard. Robust taboo search for the quadratic assignment problem. *Parallel computing*, 17(4-5):443–455, 1991.

- Zvi Drezner. A new genetic algorithm for the quadratic assignment problem. *INFORMS Journal on Computing*, 15(3):320–330, 2003.
- Tabitha James, César Rego, and Fred Glover. Multistart tabu search and diversification strategies for the quadratic assignment problem. *IEEE TRANSACTIONS ON SYSTEMS, Man, And Cybernetics-part a: systems and humans*, 39(3):579–596, 2009.
- Fred Glover. Tabu search—part i. *ORSA Journal on computing*, 1(3):190–206, 1989.
- Roberto Battiti and Giampietro Tecchiolli. The reactive tabu search. *ORSA journal on computing*, 6(2):126–140, 1994.
- Alfonso Misevicius. A tabu search algorithm for the quadratic assignment problem. *Computational Optimization and Applications*, 30:95–111, 2005.
- Ivan Karpukhin, Foma Shipilov, and Andrey Savchenko. Hotpp benchmark: Are we good at the long horizon events forecasting? *arXiv preprint arXiv:2406.14341*, 2024.
- Zhentao Tan and Yadong Mu. Learning solution-aware transformers for efficiently solving quadratic assignment problem. *arXiv preprint arXiv:2406.09899*, 2024.